Synthesis of Gold Nanoparticles within Silica Monoliths through Irradiation Techniques using Au(I) and Au(III) Precursors

Matteo Tonelli[†‡°], Sylvia Turrell[‡], Odile Cristini[†], Hicham El Hamzaoui[†], Bruno Capoen[†]*, Mohamed Bouazaoui[†], Massimo Gazzano[♦], Maria Cristina Cassani[◊]*

[†]PhLAM (CNRS, UMR 8523) and CERLA, Université Lille 1, Sciences et Technologies 59655 Villeneuve d'Ascq, France

[‡] LASIR (CNRS, UMR 8516) and CERLA, Université Lille 1, Sciences et Technologies 59655 Villeneuve d'Ascq, France

[♦] ISOF-CNR, c/o Dipartimento di Chimica "G. Ciamician", Università degli Studi di Bologna, Via Selmi 2, I-40126 Bologna, Italy

[◊] Dipartimento di Chimica Industriale "Toso Montanari", Università degli Studi di Bologna, Viale Risorgimento 4, I-40136 Bologna, Italy

[°]Present adress: Institut de Recherches sur la Catalyse et l'Environnement de Lyon, IRCELYON, UMR5256 CNRS-Université Claude Bernard Lyon 1, 2 avenue A. Einstein, F-69626 Villeurbanne cedex, France

Supporting Information

1-Synthesis of the gold precursors

(Triphenylphosphine) gold chloride.

The synthesis of $(PPh_3)AuCl$ followed a published procedure.[1]

In a typical synthesis, 1.50 mmol of $HAuCl_4 \cdot 3H_2O$ were transferred into a 100 ml round-bottomed flask and dissolved in 10 ml of ethanol. 3.20 mmol of triphenylphosphine was added drop-wise to this solution under constant stirring, leading to the immediate formation of $(PPh_3)AuCl$ as a white precipitate. The product was subsequently filtered with a sintered funnel, washed three times with ethanol and finally dried for several hours under vacuum.

Tetrabutylammonium tetrachloroaurate.

The synthesis of $[^nBu_4N][AuCl_4]$ followed a published procedure.[2]

3.10 mmol of $HAuCl_4 \cdot 3H_2O$ were dissolved in 40 ml of a 0.1 M HCl solution. Successively an aqueous solution of tetrabutylammonium chloride was prepared by dissolving 4.00 mmol of $[^nBu_4N]Cl$. This latter was added drop-wise leading to the immediate formation of a yellow precipitate. After stirring for 30 min, the precipitate was filtered on a sintered funnel, washed first with distilled water, then three times with 10 ml of diethyl ether and finally vacuum dried for several hours.

2- XRD data for the Au(I)-doped samples

Whereas for all Au(III)-doped samples, the collected XRD data showed the typical pattern of fcc gold with the expected intensities ratios of the reflections, in two cases of irradiation employing the Au(I) doped matrices (at 266 and 800 nm), the (111) reflections were overestimated in respect to the others (see Fig. 1S and 2S). No such difference in the intensities of the reflexions was observed instead for the Au(I)-doped samples irradiated at 532 nm or with the UV mercury vapor lamp (Fig. 3S and 4S respectively).

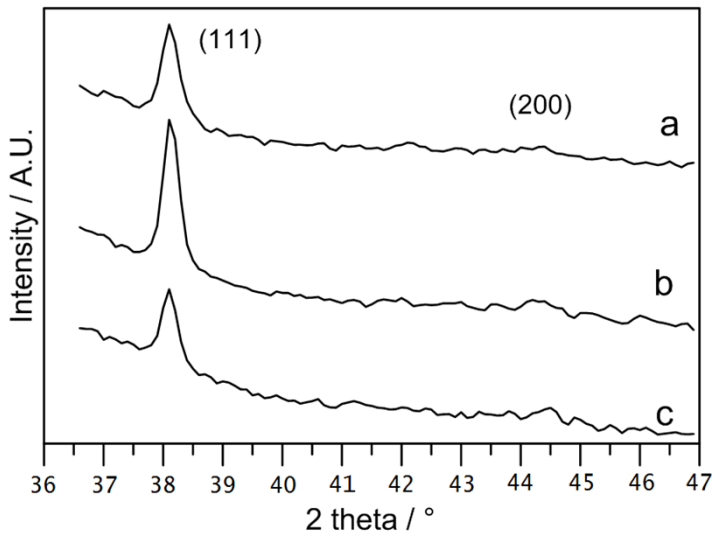

Fig. 1S Enlarged view of the (*111)* and (*200)* reflections in the XRD pattern of the Au(I)-doped samples irradiated at a) 20 mW b) 30 mW and c) 60 mW with the femtosecond pulsed laser operating at 800 nm.

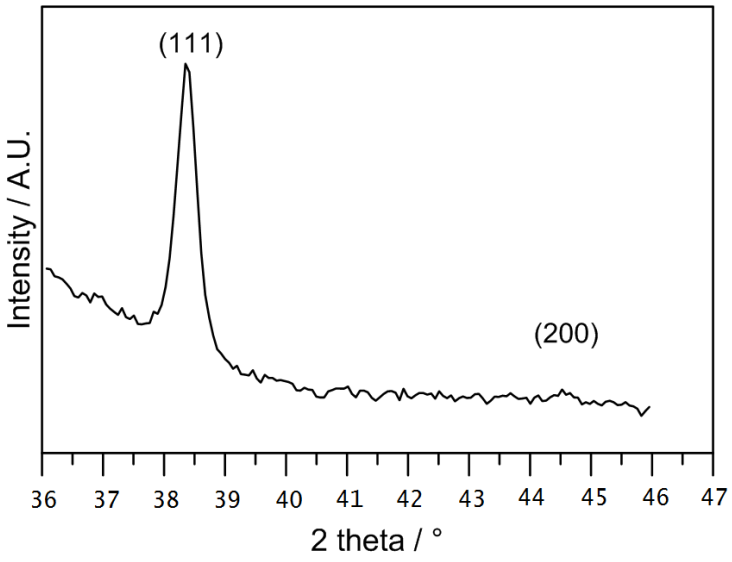

Fig. 2S Enlarged view of the (111) and (200) reflections in the XRD pattern of a Au(I)-doped sample after irradiation at 266 nm.

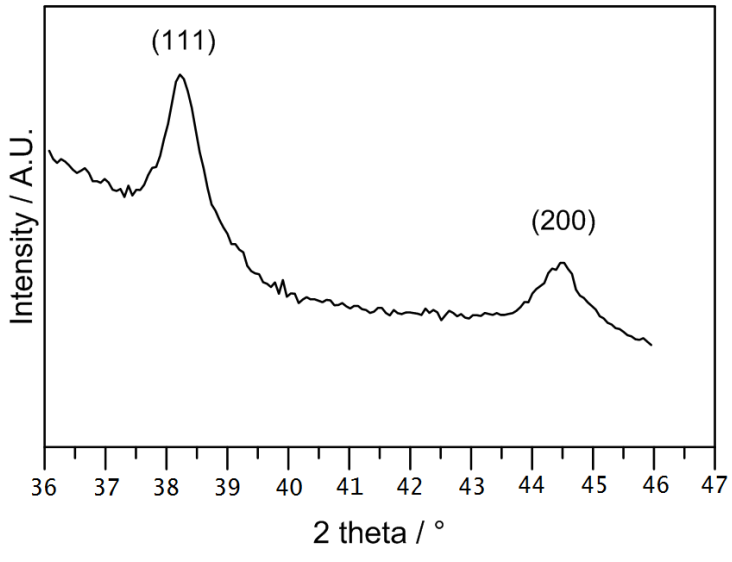

Fig. 3S Enlarged view of the (111) and (200) reflections in the XRD pattern of the Au(I)-doped after irradiation at 532 nm.

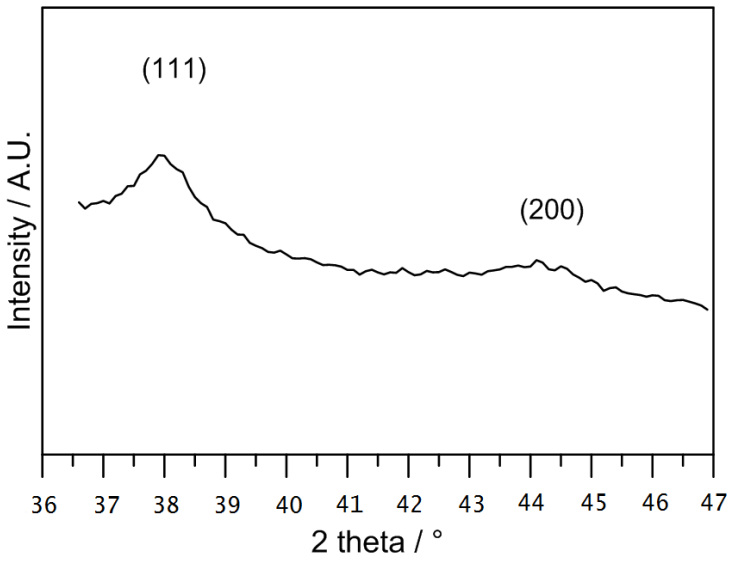

Fig. 4S Enlarged view of the (111) and (200) reflections in the XRD pattern of the Au(I)-doped sample irradiated with the UV-mercury vapor lamp.

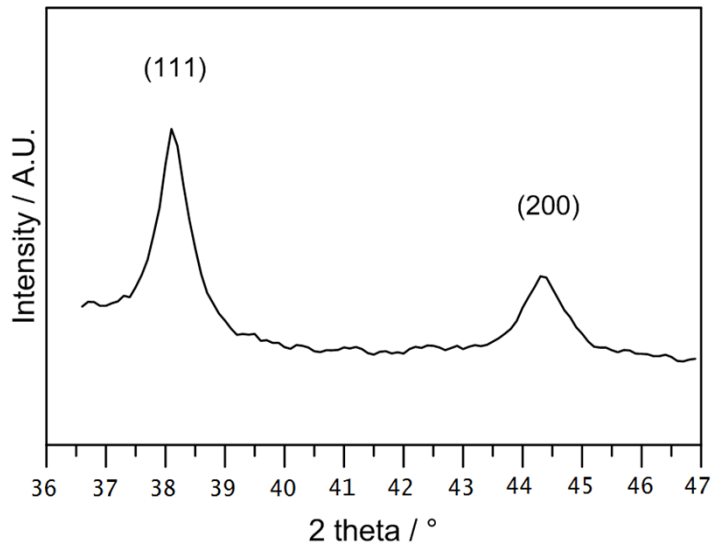

Fig. 5S Enlarged view of the (111) and (200) reflections in the XRD pattern of the Au(III)-doped sample irradiated with the laser operating at 532 nm.

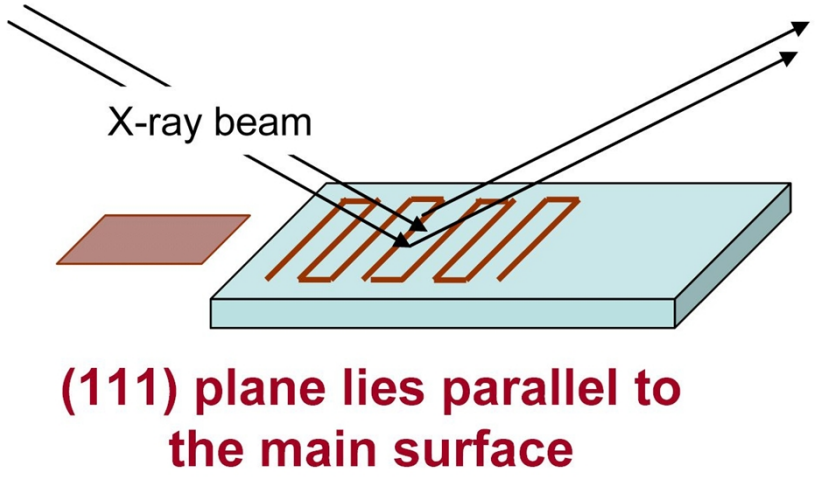

Sketch 1. Representation of the geometry used in XRD data collection. In the samples where a preferential orientation was observed, GNPs were grown with the (111) plane lying parallel to the main surface of the sample.

3- Characterization of the precursors and of the doped matrices

UV–Vis absorption spectroscopy

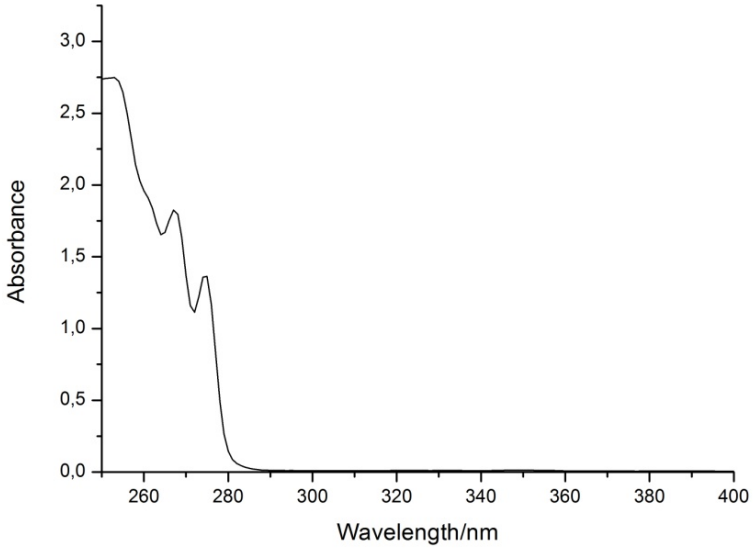

Fig. 6S UV-vis absorption spectrum of a $2 \cdot 10^{-4}$ M $(Ph_3P)AuCl$ solution in CH_2Cl_2.

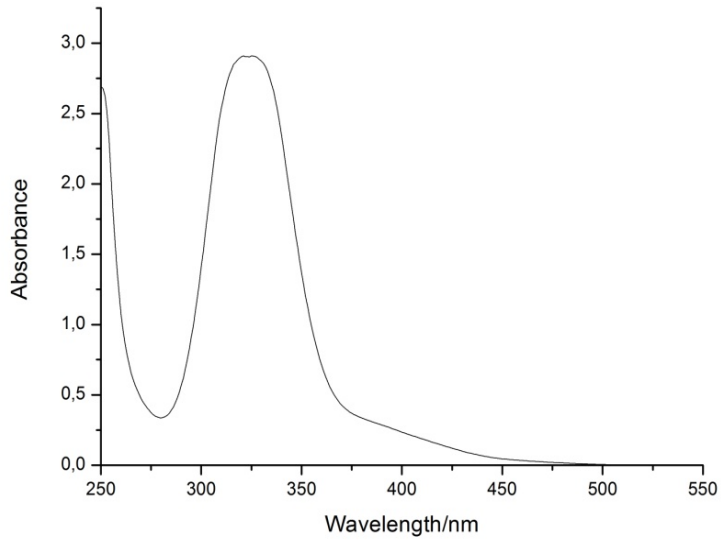

Fig. 7S UV-vis absorption spectrum of a $4 \cdot 10^{-4}$ M $[^{n}Bu_4N]AuCl_4$ solution in CH_2Cl_2.

Raman spectroscopy

The Raman spectrum characteristic of the silica xerogels used for these experiments is presented in Fig. 8S. It exhibits the well-known bands mainly dominated by a broad band around 430 cm^{-1} assigned to the δ-SiOSi network deformation[3]. The defect-mode bands D_1 and D_2, observed respectively at 495 and 606 cm^{-1}, are significantly more intense than in densified silica matrices. This observation, combined with the absence of a low-frequency band (the Boson Peak), characteristic of a vitreous dense structure, confirm that the silica matrix is still porous after the final heat treatment at 850°C.

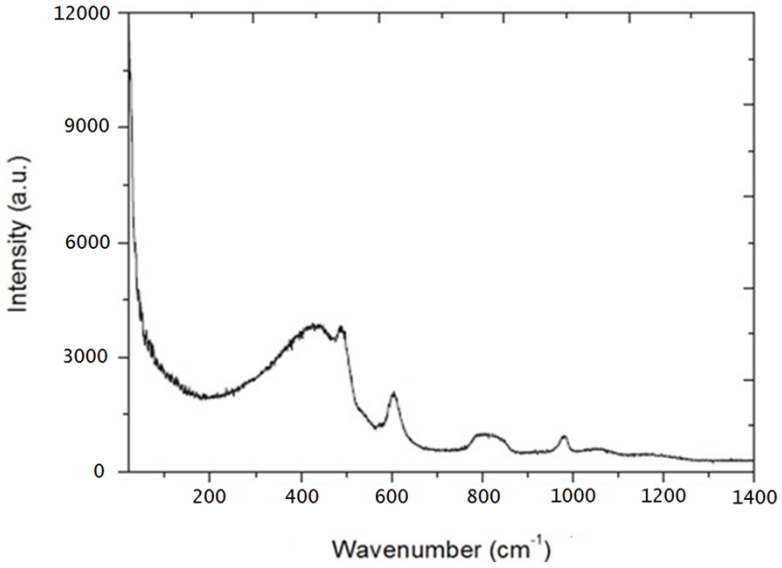

Fig. 8S Raman spectra of the silica xerogel stabilized at 850°C.

In Fig. 9Sa, the Raman spectrum of the xerogel after impregnation with the Au(I) precursor is presented. The three bands characteristic of vibrations of the phenyl ring of [AuCl(Ph_3P)] (Fig. 9Sb) are superposed on the signal of the silica matrix, confirming the presence of the precursors within the matrix. The most intense band at 999 cm^{-1} has been previously assigned[4,5] to the ring breathing of the phenyl group. The band at 1028 cm^{-1} corresponds to the in-plane bending vibration of the C-H in the phenyl ring and finally the weaker band at 1103 cm^{-1} arises from the stretching of the P-C(Ph) bond[4].

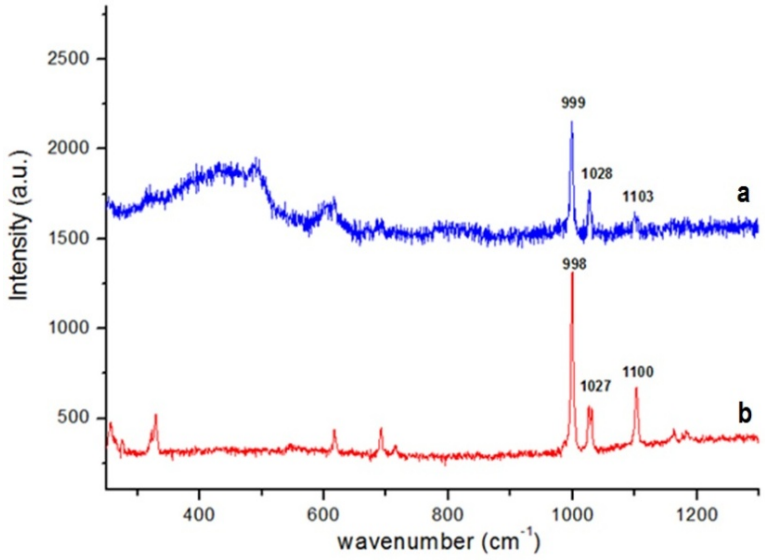

Fig. 9S a) Raman spectrum of the matrix impregnated with the Au(I) precursor b) Raman spectrum of $(Ph_3P)AuCl$. Experimental conditions: λ_{exc} = 632.8 nm; Accumulation time: 20 s; Number of accumulations: 4.

The Raman spectrum of $[^nBu_4N][AuCl_4]$, shown in Fig. 10Sb, is characterized by three bands centred at about 340 cm^{-1}. The most intense peaks at 323 and 347 cm^{-1} are associated with the ν_2 (B_{1g}) and ν_1 (A_{1g}) vibrations of the square planar $[AuCl_4]^-$ ion, respectively[5]. These bands are clearly visible in the spectrum of the impregnated sample (Fig. 10Sa) together with the signal of the silica matrix, proving that the $[^nBu_4N][AuCl_4]$ molecules have maintained their structure.

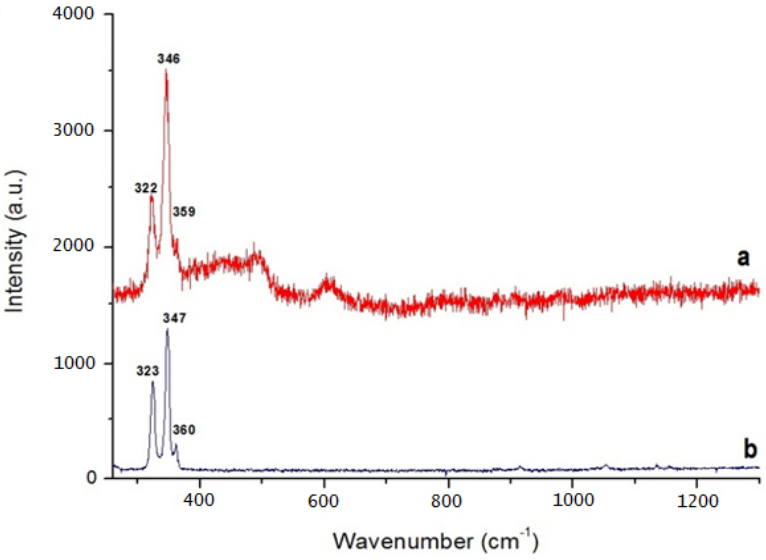

Fig. 10S a) Raman spectrum of the matrix impregnated with the Au(III) precursor b) Raman spectrum of $[^{n}Bu_4N][AuCl_4]$. Experimental conditions: λ_{exc} = 632.8 nm; Accumulation time: 20 s; Number of accumulations: 4.

Thermal Gravimetric Analysis (TGA)

TGA profiles were collected in air on a SETARAM SETSYS Evolution 18 instrument with a heating rate of 10°C/min and making use of platinum crucibles. TGA data indicate that for both precursors, the decomposition starts at about 220°C. A mass loss of 57.0 % is observed for $(Ph_3P)AuCl$ at 290°C (see Fig. 11S), which is very close to the calculated value for the formation of elemental gold (60.2%).

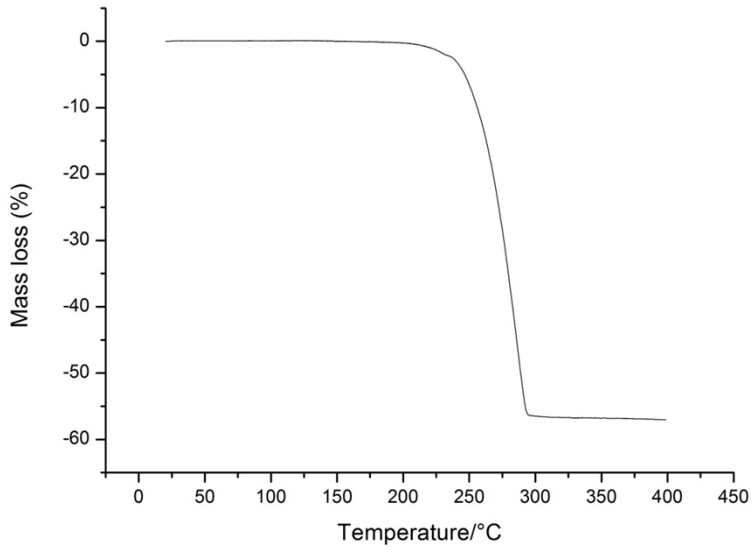

Fig. 11S TGA performed on 7.3 mg of $(Ph_3P)AuCl$.

Also in the case of $[^nBu_4N][AuCl_4]$, reported in Fig. 12S, it is possible to conclude that the last step of the thermal decomposition leads to elemental gold, as the final mass loss (64.8%) is very close to the calculated value required for gold formation (66.1%).

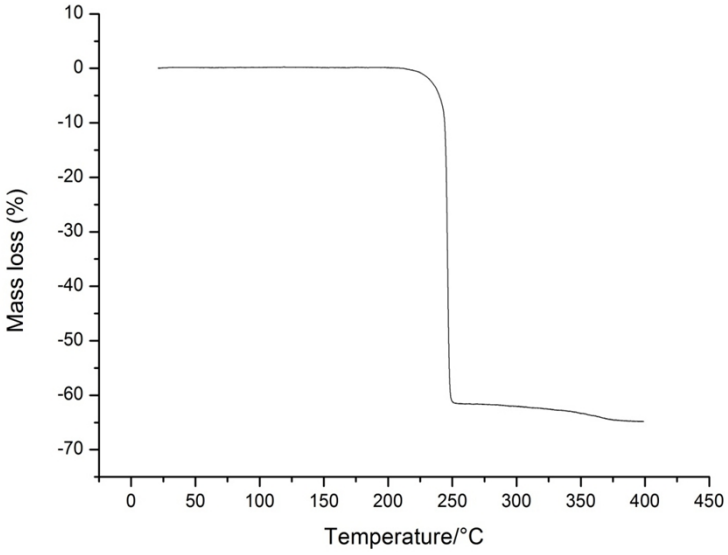

Fig. 12S TGA performed on 4.4 mg of $[^nBu_4N][AuCl_4]$.

References

1 N. J. Destefano and J. L. Burmeister, *Inorg. Chem.*, 1971, **10**, 998–1003.

2 S. L. Barnholtz, J. D. Lydon, G. Huang, M. Venkatesh, C. L. Barnes, A. R. Ketring and S. S. Jurisson, *Inorg. Chem.*, 2001, **40**, 972–976.

3 C. J. Brinker and G. W. Scherer, *Sol-Gel Science: The Physics and Chemistry of Sol-Gel Processing*, Gulf Professional Publishing, 1990.

4 R. Faggiani, H. E. Howard-Lock, C. J. L. Lock and M. A. Turner, *Can. J. Chem.*, 1987, **65**, 1568–1575.

5 Y. M. Bosworth and R. J. H. Clark, *Inorg. Chem.*, 1975, **14**, 170–177.